Int. J. Multiphase Flow Vol. 19, No. 6, pp. 999–1012, 1993
Printed in Great Britain.

0301-9322/93 $6.00 + 0.00

OFF-SITE CALIBRATION OF A TWO-PHASE PATTERN RECOGNITION FLOWMETER

N. A. BEG† and H. TORAL
Department of Mineral Resources Engineering, Imperial College of Science, Technology and Medicine, Prince Consort Road, London SW7 2BP, England

(Received 10 January 1992; in revised form 11 August 1993)

Abstract—A technique is presented for the measurement of individual phase flowrates in two-phase flow without separation. The technique is based on signal analysis and pattern recognition methodologies to extract, classify and identify stochastic features from turbulent pressure waveforms. Experiments in a horizontal air–water loop have shown that a set of features is uniquely related to the individual phase flowrates. It is shown that the "flowmeter" can be isolated from installation effects by means of a homogenizer.

Key Words: horizontal gas–liquid flow, pattern recognition, two-phase flowmeter, installation effects, flow homogenizer

1. INTRODUCTION

1.1. Background

There are a number of studies in which pressure and void fraction waveforms have been analysed by stochastic methods to discriminate between different flow patterns (Vince & Lahey 1982; Matsui 1985; Sekoguchi *et al.* 1987; King *et al.* 1988; Lu & Wang 1991).

The present technique is founded on the premise that the turbulence characteristics of multiphase flow are uniquely related to the flowrates of the individual phases in a given pipe under given conditions. The stochastic treatment of the turbulent pressure waveforms was enhanced by applying signal analysis methods employed in other disciplines, such as voice recognition and seismic analysis. "Stochastic features" were extracted from proprietary pressure sensors, and classified and related to the individual flowrates of the phases.

In our previous studies, Darwich *et al.* (1991) demonstrated that the technique can offer a high accuracy over a wide range of flow regimes in horizontal two-phase flow, provided that it could be calibrated on-site. The present study was conducted to examine installation effects on the calibration database with a view to the elimination of the previously perceived prerequisite for on-site calibration.

Figure 1 shows a schematic diagram of the two-phase flow measuring technique, which comprises the principal procedures:

(i) Removal of high-frequency noise by using a low-pass analog filter.
(ii) Digitize and store the hydrodynamic waveform (e.g. differential pressure signal).
(iii) Extract the "feature-set" from the waveform.
(iv) Categorize the "feature-set" by pattern identification against the "calibration database (of feature-sets)".
(v) Uniquely relate the category to a grid cell on the superficial gas vs liquid flowrate domain.

1.1.1. Features

Raw time-domain signals do not easily lead themselves for "interpretation" or "classification". It is advantageous to represent the signal in the form of features, which take less storage space and contain all the characteristics of the parent source. In pattern recognition/identification of unknown input where extensively large calibration on a raw signal would mean a slow response, properly selected features would result in a rapid response and a higher recognition accuracy.

†Present address: CALtec Ltd (BHR Group Ltd), Cranfield, Bedford MK43 0AJ, U.K.

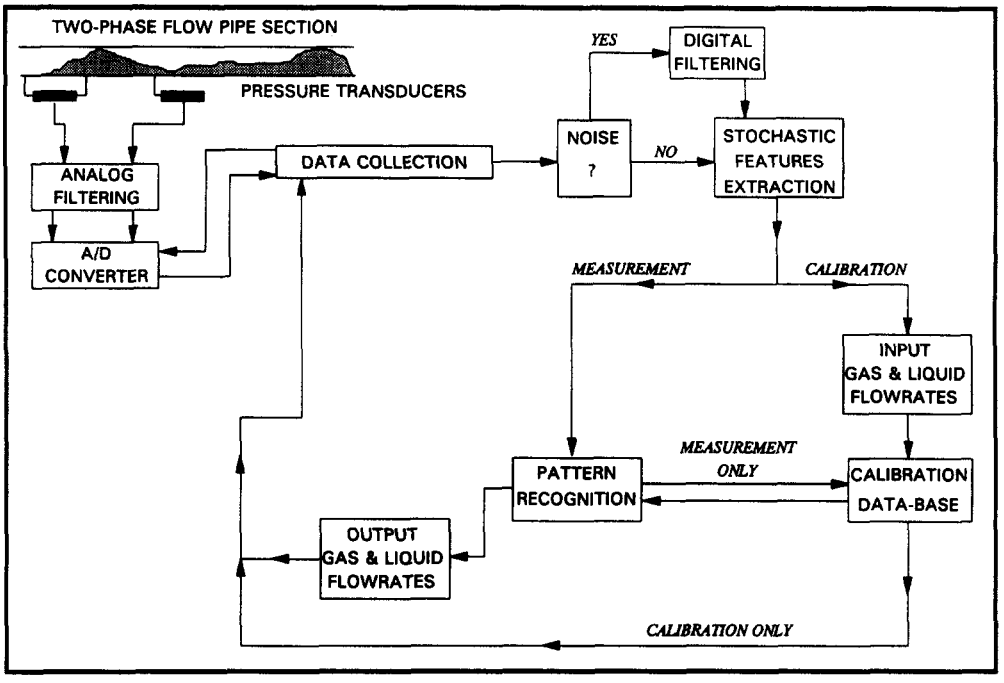

Figure 1. Schematic representation of flowrate measurement.

The following feature-set was derived from the pressure waveform:

$$[SD \quad CS \quad CK \quad Ep \quad A_1 \quad A_2 \quad A_3 \quad A_4] \qquad [1]$$

where the first three elements can be described as amplitude domain features, namely standard deviation (SD), coefficient of skewness (CS) and coefficient of kurtosis (CK). They serve the purpose of capturing Gaussianly (or non-Gaussianly) distributed statistical properties of the signal. Any book of statistics can reveal the equations regarding these three features.

The remaining five elements are the frequency-domain features obtained from a popular method in speech processing and recognition known as linear prediction. In brief, this method extracts the main frequency-domain characteristics of the signal. The signal is modelled as a linear combination of its past values and past and present values of a hypothetical input to a system whose output is the given signal. The predictor coefficients ($A_1 \cdots A_4$) are selected on the basis of the minimum residual error Ep which results from the difference between the actual and the predicted signal. Makhoul (1975) has given a through review of the linear prediction method.

1.1.2. Categorizer

The task of the categorizer is to determine the closeness of the match between an unknown feature-set and calibration database (composed of known flow-conditions feature-sets) to recognize and uniquely relate gas and liquid flowrates to that unknown feature-set. This type of recognition (matching) is known as template-matching pattern recognition, which measures the Euclidean distance between two vectors. The Euclidean distance is given as

$$D^i = \left\{ \sum_{j=1}^{m} \left(\frac{U_j - C_j^i}{R_j} \right)^2 \right\}_{i=1,n}. \qquad [2]$$

Where D^i is the Euclidean distance determined between the unknown feature-set U and the ith calibration feature-sets C^i (n is the total number of feature-sets in a calibration database). The best match between the calibration vector C^i and the unknown vector U corresponds to the minimum value of D^i. U_j and C_j are the jth feature of the unknown and calibration vector, respectively, and m is the number of features used. In this investigation, equal weights were assigned to all features in the feature-set. R_j is the range of the jth feature in the entire calibration

database used for normalization, in order to force the dynamic ranges of features to be well represented.

1.1.3. Accuracy

The measuring accuracy (recognition) of the flowrate measurement technique was assessed on an error measure similar to the one defined by Ashkuri & Hill (1985), Kouba *et al.* (1990), Darwich *et al.* (1991) and Mazzoni *et al.* (1991) to assess the performance of their proposed multiphase flowmeters.

The error measure (Er) for the individual measurements can be defined as

$$Er = \frac{V_a - V_m}{V_{max} - V_{min}} \times 100, \quad [3]$$

where V_a is the actual superficial velocity, V_m is the recognized superficial velocity and $V_{max} - V_{min}$ is the measurable flow range of each phase. A measurement is considered successful if it falls within a $\pm 10\%$ error band (Er). A percentage of the total successful measurements was used to describe the accuracy of the flowmeter.

2. QUANTIFICATION CRITERIA

2.1. Similarity Scale

The measuring accuracy depends on the reproducibility of the feature database. In this study a method named the "Similarity Scale" has been proposed. The degree of reproducibility can be quantified by the "Similarity Scale" (provided the feature-set is the same).

As in any comparison criteria, the data-sets under comparison should be collected at the same reference points with the same number of observations. In practical situations, however, this criterion is not an easy task to meet. Therefore, to overcome this problem, data is selected on a common range of superficial gas and liquid velocities and the feature values are interpolated over the same grid cells. The proposed quantification method was derived from the Euclidean distance measures where the Similarity Scale S between two data-sets P and Q is defined by

$$S = \frac{1}{M} \sum_{j=1}^{M} \sqrt{\frac{1}{N} \sum_{i=1}^{N} \left(\frac{P_i^j}{P_{max}^j} - \frac{Q_i^j}{Q_{max}^j} \right)^2}, \quad [4]$$

where P_i^j and Q_i^j show the ith grid-cell value (Z-elevation) for the jth feature and P_{max}^j and Q_{max}^j are the maximum grid-cell values (for the jth feature). M represents the total number of features and N is the total number of grid cells compared. Dividing by the terms N and M standardizes the Similarity Scale to range between "0" (i.e. both data-sets are identical) and "1" (the data sets are completely different).

For all other values between "0" and "1", the Similarity Scale gives a relative measure of the degree of similarity between the respective data pairs drawn out of a closed data-set group. Thus, a higher measuring accuracy would be expected for a data pair with an S value closer to "0".

2.2. F-ratio

In order to evaluate the selected statistical features in terms of their ability to discriminate the different flow conditions over the ranges of superficial gas and liquid velocities investigated in this study, the F-ratio commonly used in pattern recognition, was implemented. For a single statistical feature, the F-ratio equation will be

$$F - ratio = \frac{variance\ of\ the\ flow\ condition\ means}{average\ within\ flow\ condition\ variance}. \quad [5]$$

A suitable feature for recognition is one for which [5] has a higher value for the numerator than for the denominator. In other words, the distribution of the different flow conditions are concentrated at widely different locations in the feature space. Consequently, the more suitable the

feature, the higher the value of the F-ratio. A good mathematical description of the F-ratio is given by Atal (1976).

3. DESCRIPTION OF THE EXPERIMENTS

3.1. Test Rig

A schematic diagram of the horizontal two-phase flow loop is shown in figure 2 with its overall dimensions.

As shown in figure 2, installation effects were studied for four different geometric "configurations" where configuration I is a plain pipe, configuration II is a pipe with a constriction at its inlet, configuration III is a pipe with a homogenizer at its inlet and configuration IV is a pipe with a constriction and a homogenizer at its inlet. Each configuration was made of a 5 cm diameter pipe with an orifice plate (3.75 cm) located at a distance of 6.2 m from the inlet of the section and fitted with a differential pressure sensor and an absolute pressure sensor ("detection sensors"). Toral *et al.* (1990) have shown that the discriminating strength of the features was further enhanced by the presence of an orifice plate in the two-phase pipe.

The homogenizer, a Statiflo motionless model (Type 2″ NB 4 elements), was used. The purpose of the homogenizer was to isolate the detection sensors from upstream installation effects. However, since the accuracy of the present technique is dependent on the presence and characterization of naturally occurring multiphase flow turbulence, the flow must be allowed to redevelop downstream of the homogenizer before reaching the detection sensors. The optimum downstream location of the orifice plate around which the detection sensors were placed was determined by visual observation of the established flow patterns which remained unchanged to the end of the two-phase pipe section. The redeveloped flow is not the same as the flow patterns upstream of the homogenizer. A quantitative study is proposed with reference to the technique's internal signal strength characterization procedures and Similarity Scale but such a study has not yet been conducted.

Water flowrate was measured with an orifice and the compressed air flowrate was measured with a rotameter and/or an orifice. The data range collected on the superficial gas and liquid velocities

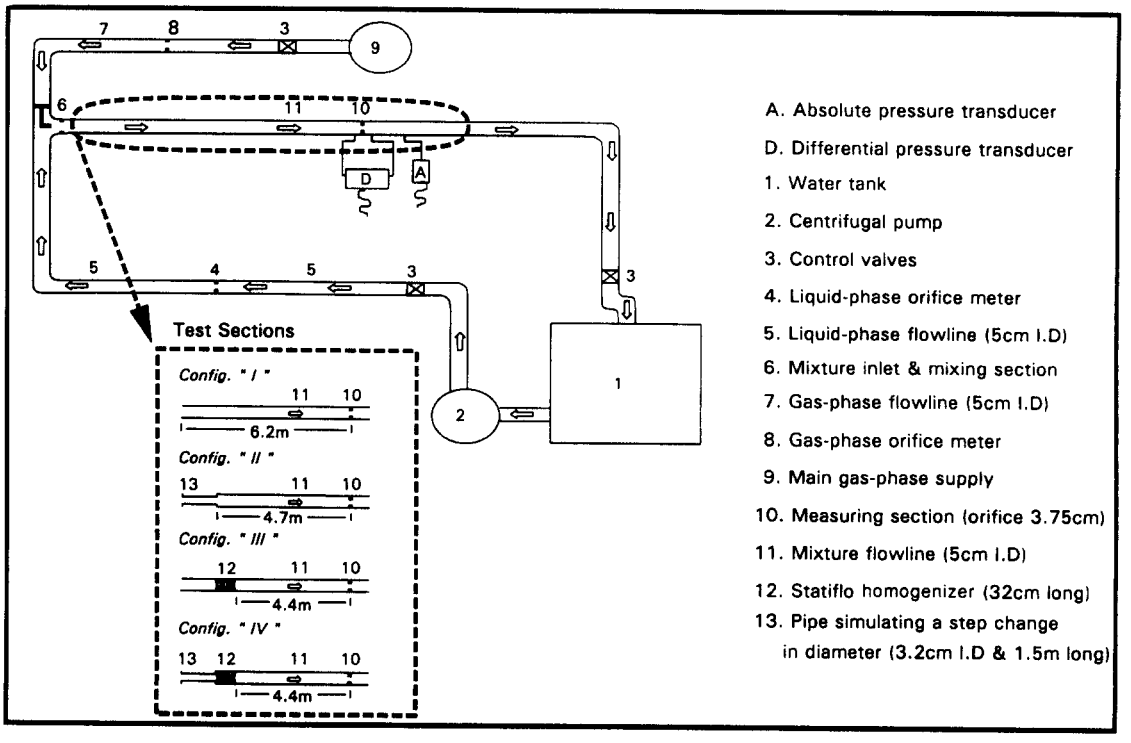

Figure 2. Air–water two-phase flow loop and test section configurations.

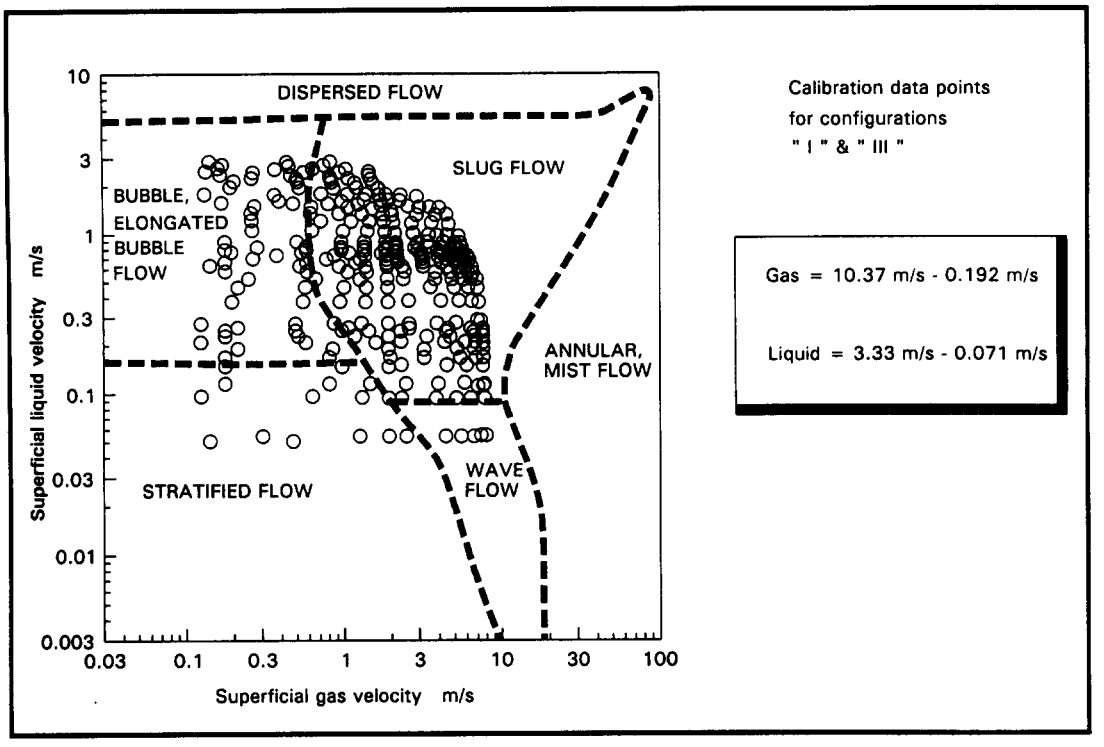

Figure 3. Range of the gas and liquid superficial velocities.

and flow patterns [on a Mandhane *et al.* (1974) map] are shown in figure 3. The major portion of the data was obtained in the slug flow regime because of its dominating occurrence and importance in the petroleum industry. All measurements were carried out at near-atmospheric conditions.

3.2. Detection Sensors

The test section was fitted with an absolute pressure and a differential pressure sensor. The differential pressure sensor was installed across an orifice plate with tappings placed 2.5 cm both upstream and downstream. The absolute pressure was installed 10 cm downstream of the orifice. Figure 2 shows schematically the positions of installation.

3.3. Data Acquisition System

Measurements were digitized with an analog-to-digital (A/D) converter controlled by a personal computer. The A/D converter employed a 12-bit digitizer with a maximum sampling frequency of 20 kHz through one channel and through 8 channels at a lower sampling frequency. Waveforms could be displayed on the screen in the time domain or in the frequency domain. Digitial filtering software allowed the design and implementation of lowpass, highpass, bandpass and bandstop recursive or nonrecursive filters to isolate extraneous noise from the sampled waveforms. The spectral density of the signals was displayed to determine the optimum sampling frequency and record lengths.

4. RESULTS AND DISCUSSION

In the first part of the study configurations I–IV were used to assess the technique's accuracy with on-site calibration. In the second part, operation in the off-site calibration mode was simulated by carrying out measurements in "disturbed configurations" against calibration databases obtained from straight pipes. In the final part of the study the effect of the homogenization in eradicating the off-site calibration deviations was studied.

To summarize, the following series of tests were devised:

Test 1. On-site calibration (repeatability tests of configurations I vs I and III vs III).
Test 2. Off-site calibration without a homogenizer (reproducibility test for configurations II vs I).
Test 3. Off-site calibration with a homogenizer (reproducibility test for configurations IV vs III).

4.1. Test 1. On-site Calibration

Measurements in this series were designed to evaluate the repeatability accuracy of the technique used with an on-site calibration database. Accuracy tests were conducted in each one of the configurations. For brevity, the procedure followed in the tests is explained once in this section and will not be repeated when discussing Tests 2 and 3.

4.1.1. Calibration

Absolute pressure and differential pressure waveforms were sampled and analysed on a total of 367 points for configuration I and 303 points for configuration III. Each measurement comprised 4096 sample points, divided into 16 blocks of 256 points to test for statistical stationarity. The waveform variations were graphically studied, in the time-domain and frequency-domain, to detect extraneous noise. The noise in this context means the frequency ranges with no significant information and the dominant 50 Hz mains electrical supply embedded in the signals. It was eliminated by analog and digital filtering.

The feature-sets (see section 1.1.1.) were derived from each pressure waveform. A preliminary study of the stationarity of the waveforms was made by plotting the average value of the features within a sample block of 256 points over 16 blocks (figure 4). Figure 4 shows the strength of a single feature (*SD*) to discriminate among different flow patterns (or superficial velocity pairs). In the same manner, other features also responded differently to differentiate not only flow regimes but also the change in superficial velocities within a single flow regime. Therefore, the joint effect of all 8 features was used in this technique for flowrate determination.

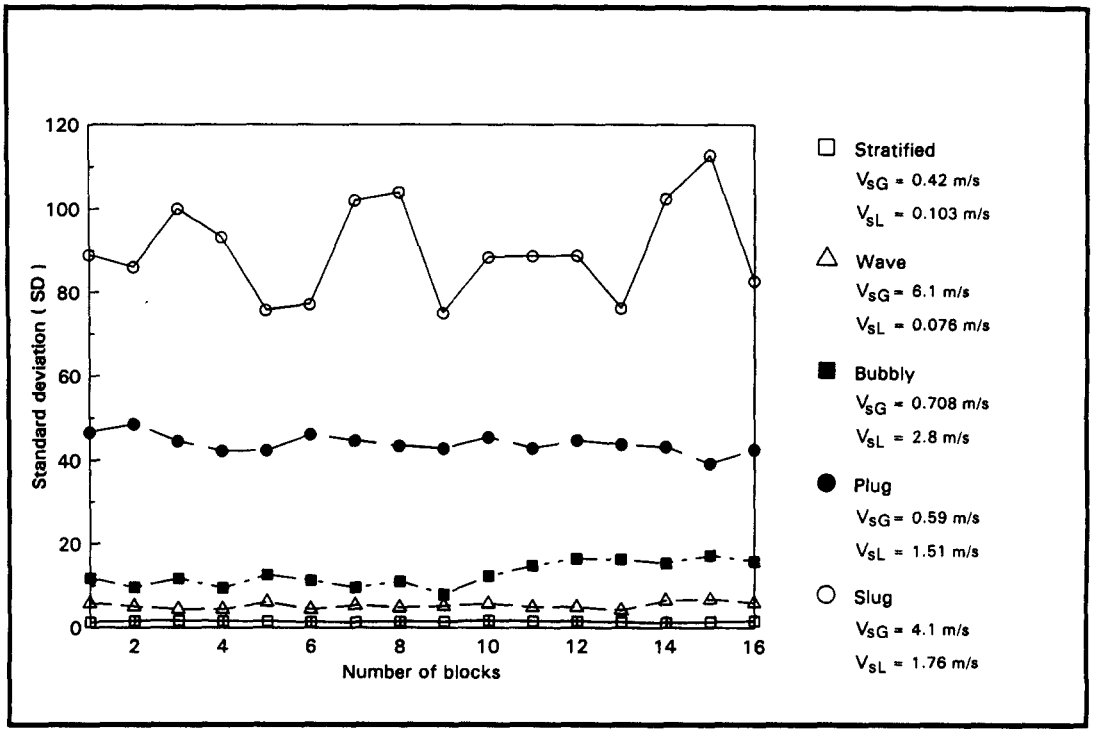

Figure 4. Variation of the differential pressure signal feature *SD* with the sample block and flow regimes.

Feature-set measurements were surface fitted over a 40×40 regular grid cell by contouring techniques. Figure 5 shows the distribution (contour map) of a single feature (SD) for the differential pressure signals for configurations I and III, respectively, over the superficial velocity domain. This gives a clear picture of the feature response over the investigated range with multiple measurements within a single flow regime. The feature value shows a gradual ascent on either side of the flow regime labelled transition boundaries when one flow regime is taken over by another flow regime. This indicates that there are no boundaries between flow regimes when viewed through these features. Similar maps were also drawn for each one of the features. Values of the features were interpolated for the grid cells from the contour maps ("the calibration database"). Figure 6 gives a conceptual representation of the feature-set as a "unique multidimensional object" for each grid cell.

The contour maps obtained from configurations I and III showed similar trends in the two configurations but the isolines did not coincide on the superficial velocity surface, demonstrating the difference between both calibration databases which is dependent on installation effects (i.e. the installation effect created by the presence of a homogenizer). The difference between the calibration databases was tested on the Similarity Scale. A value of 0.208 was obtained, indicating the degree of difference between the two calibration databases.

The feature-set strength with respect to the specific waveform (e.g. differential pressure or absolute pressure) and individual features (e.g. standard deviation, linear prediction coefficient etc.) was quantified by the F-ratio test (figure 7). In general, the differential pressure signal was found to be stronger (higher F-ratios) than the absolute pressure signal. The F-ratios seem to decrease with the introduction of a disturbance by step expansion, as in configuration II, or else the F-ratio indicates a deterioration of the potential measuring accuracy of the technique with homogenization. This finding is to be expected since our technique relies on the structural differences in the fluid dynamics of different flow regimes. If these differences are suppressed by homogenization the accuracy of the technique would deteriorate.

The F-ratio test was performed to assess the strength of the individual features of the absolute pressure and differential pressure signals. The F-ratio of configuration IV was seen to be comparable in strength to configuration III.

4.1.2. Measurement

The template-matching categorizer technique was used in the identification tests. The following feature-sets were tested: absolute pressure with 8 features; differential pressure with 8 features; absolute and differential pressure combined with 16 features. In configuration I, no appreciable improvement in the recognition rate was observed by the combination of the features from the differential pressure and absolute pressure sensors but a slight improvement was observed for configuration III.

The Similarity Scale was determined for the feature-set of configurations I vs I and configurations III vs III, which resulted in values of 0.131 and 0.159, respectively. The S values obtained from these "self similarity tests" established a datum of similarity. Thus, in the further tests applied below, S values above 0.131 and 0.159 will indicate the relative degree of dissimilarity between the data-sets under comparison. Figure 8 summarizes all three tests on the Similarity Scale. The F-ratios and the Similarity Scale values are expected to recover with downstream distance as the flow regime is recovered. Thus, the flow recovery length downstream of the disturbance should be the determining factor in obtaining the optimum location of the detection sensors. A detailed study of this type has not yet been conducted.

Figures 9 and 10 compare the accuracy of recognized (measured) against actual (reference) superficial velocities.

As expected from its strong F-ratio values, the technique resulted in a higher accuracy of measurement in configuration I compared with configuration III. The tables on the figures provide an alternative assessment of accuracy in terms of the number of measurements that fall within a $\pm 10\%$ error band (Er) as a percentage of the total measurements. The total number of measurement points is shown in the respective tables.

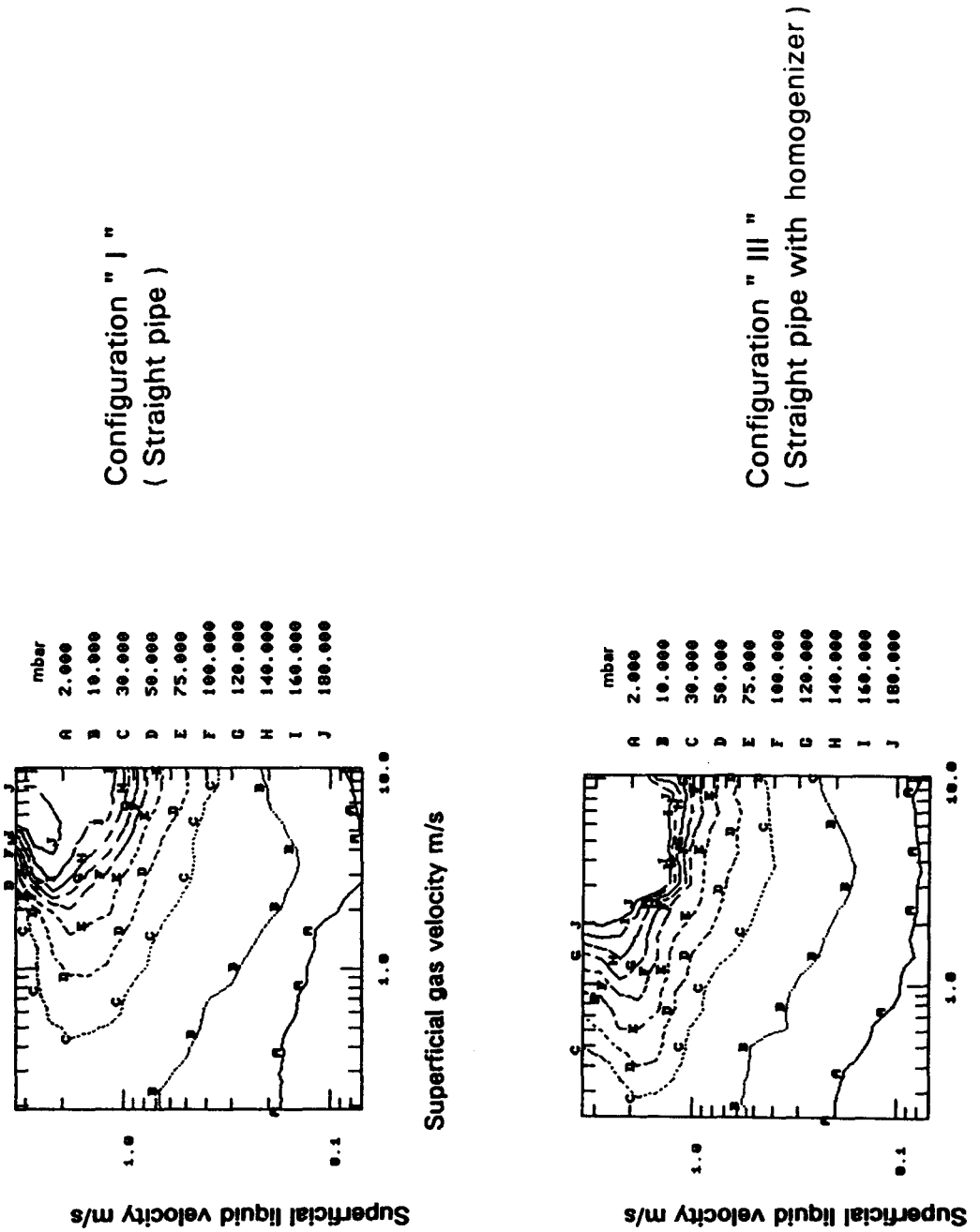

Figure 5. Calibration isolines of the differential pressure feature *SD* in Test 1 (configurations I and III).

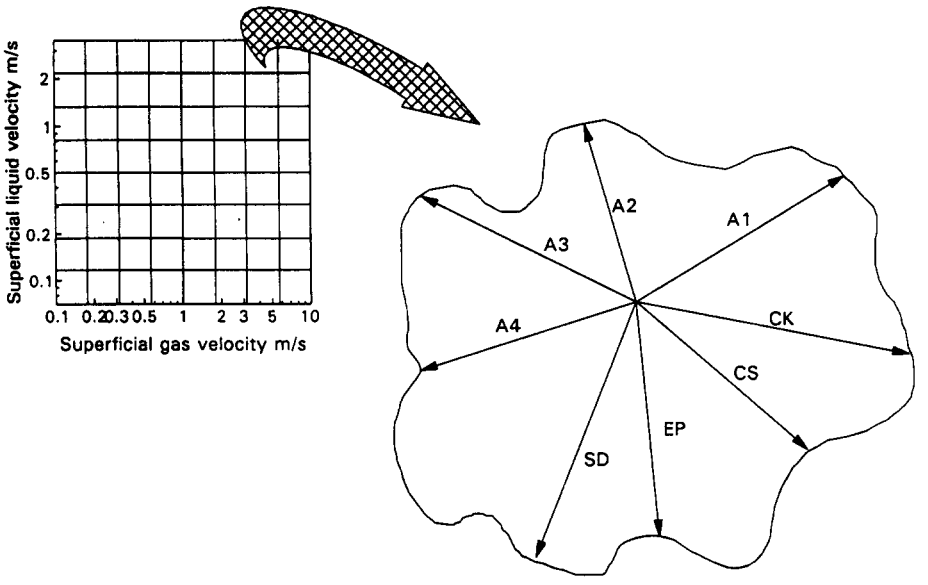

Figure 6. Feature-set—"an object" in multidimensional feature-space.

4.2. Test 2. Off-site Calibration Without a Homogenizer

Measurements in this test series were designed to evaluate the accuracy of the technique used with an off-site calibration database.

Configuration II was designed as a pipe section to simulate an upstream disturbance in configuration I. That is, configuration II is a pipe section like configuration I in all respects, except that it has a built-in disturbance. The disturbance was achieved by a step expansion at the inlet.

A set of 67 measurements was made with reference to the calibration database obtained from configuration I.

Configuration " I "

Feature	Absolute pressure	Differential pressure
SD	36.1	75.8
CS	9.3	3.5
CK	0.33	1.32
EP	3.54	2.9
A1	13.46	14.6
A2	5.14	4.78
A3	0.75	2.8
A4	1.76	2.6

Configuration " III "

Feature	Absolute pressure	Differential pressure
SD	34.8	64.45
CS	1.98	3.93
CK	0.52	2.13
EP	2.11	1.55
A1	1.00	5.83
A2	2.01	4.33
A3	2.99	1.67
A4	4.02	1.72

Configuration " II "

Feature	Absolute pressure	Differential pressure
SD	9.95	41.8
CS	3.18	3.59
CK	0.56	2.05
EP	2.42	1.6
A1	2.63	3.92
A2	3.65	2.55
A3	2.47	1.02
A4	1.3	1.27

Configuration " IV "

Feature	Absolute pressure	Differential pressure
SD	33.7	63.53
CS	3.54	5.82
CK	0.85	2.38
EP	0.73	3.16
A1	2.23	2.22
A2	2.87	1.24
A3	1.39	0.88
A4	1.11	1.29

Figure 7. Features' F-ratios for all configurations.

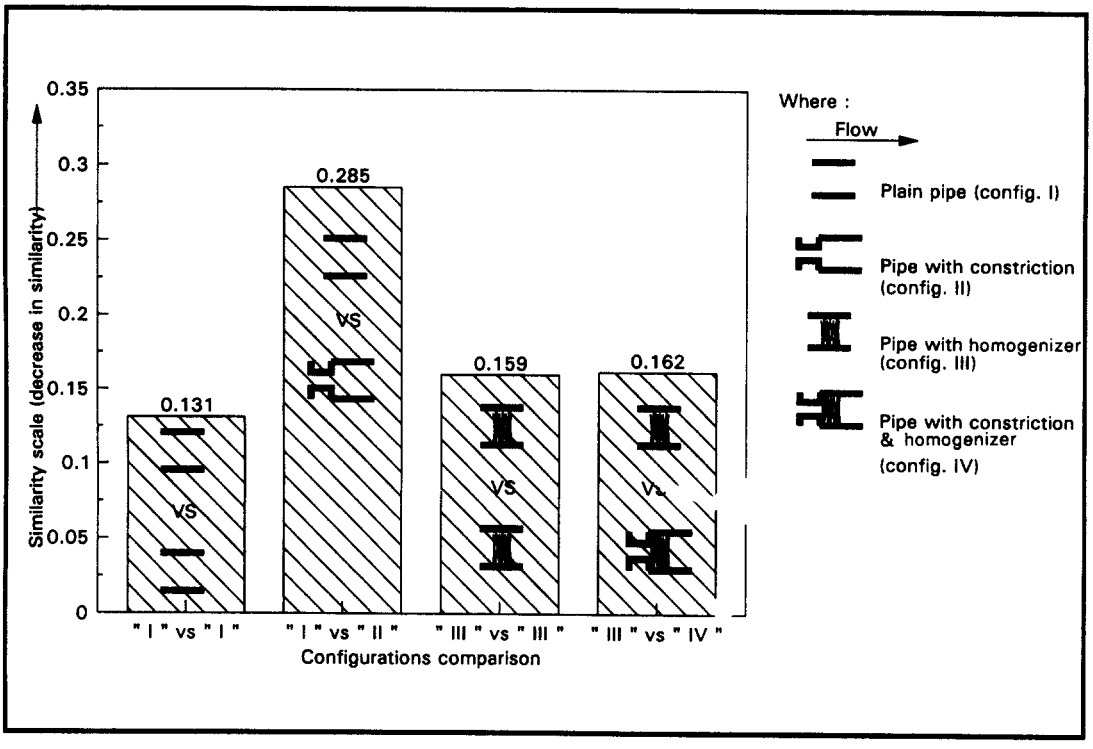

Figure 8. Configurations comparison on the Similarity Scale.

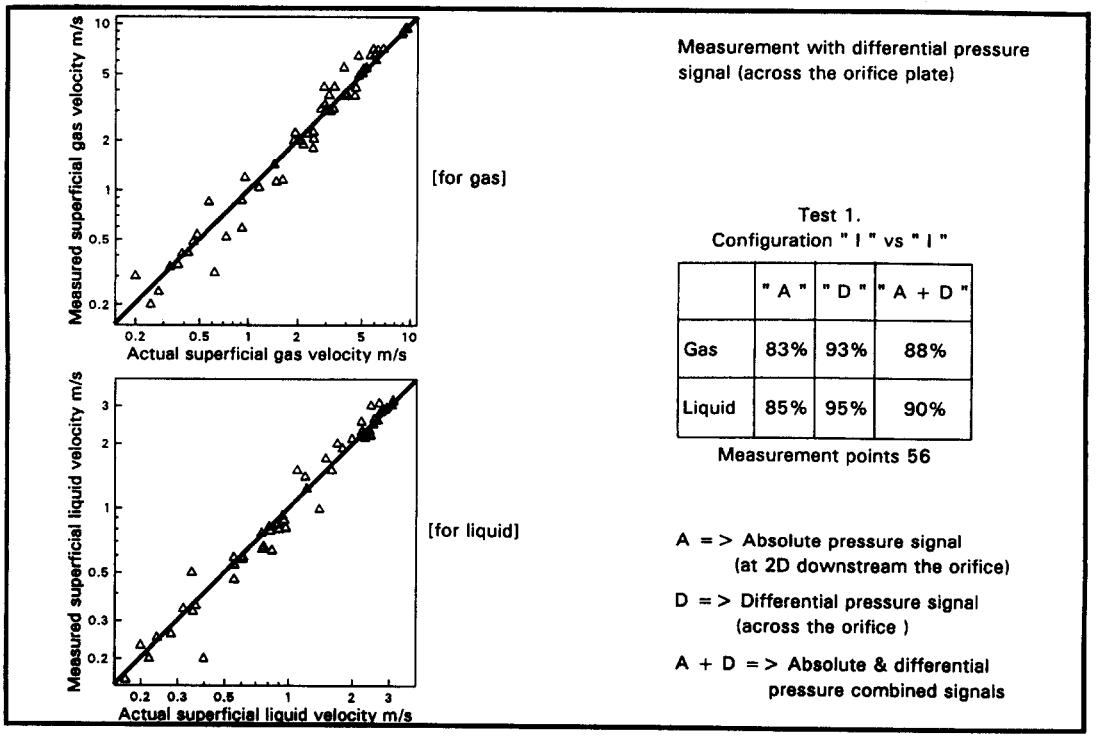

	" A "	" D "	" A + D "
Gas	83%	93%	88%
Liquid	85%	95%	90%

Figure 9. Measuring accuracy (Test 1, configurations I vs I).

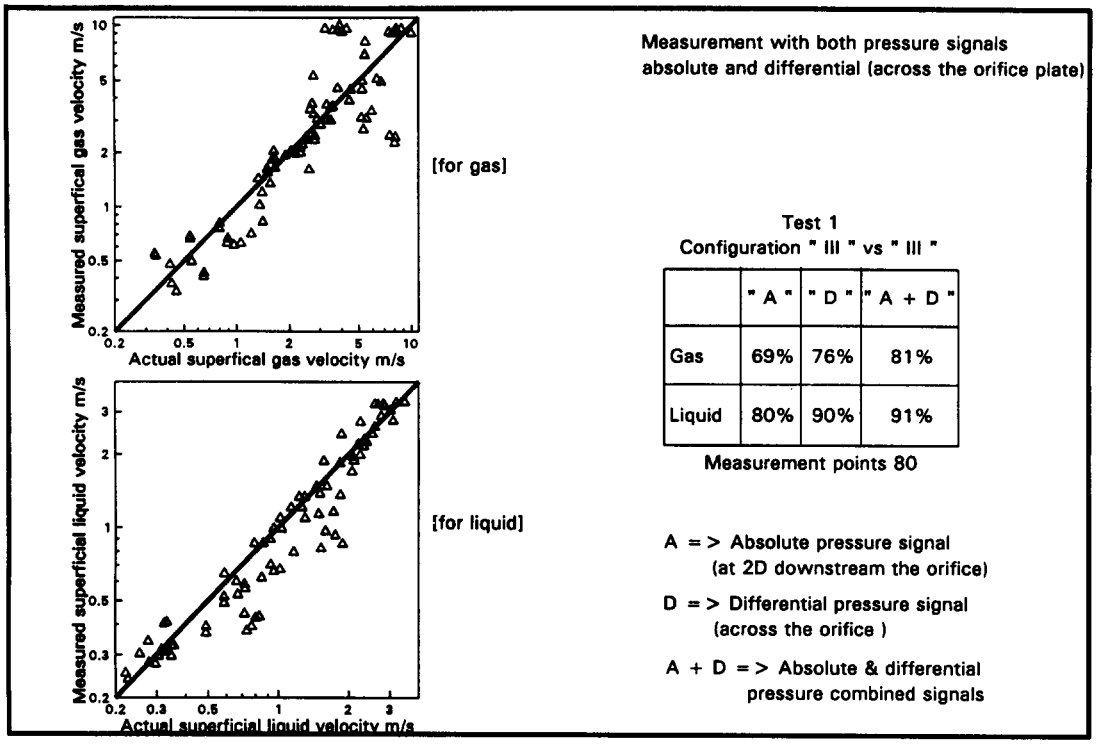

Figure 10. Measuring accuracy (Test 1, configurations III vs III).

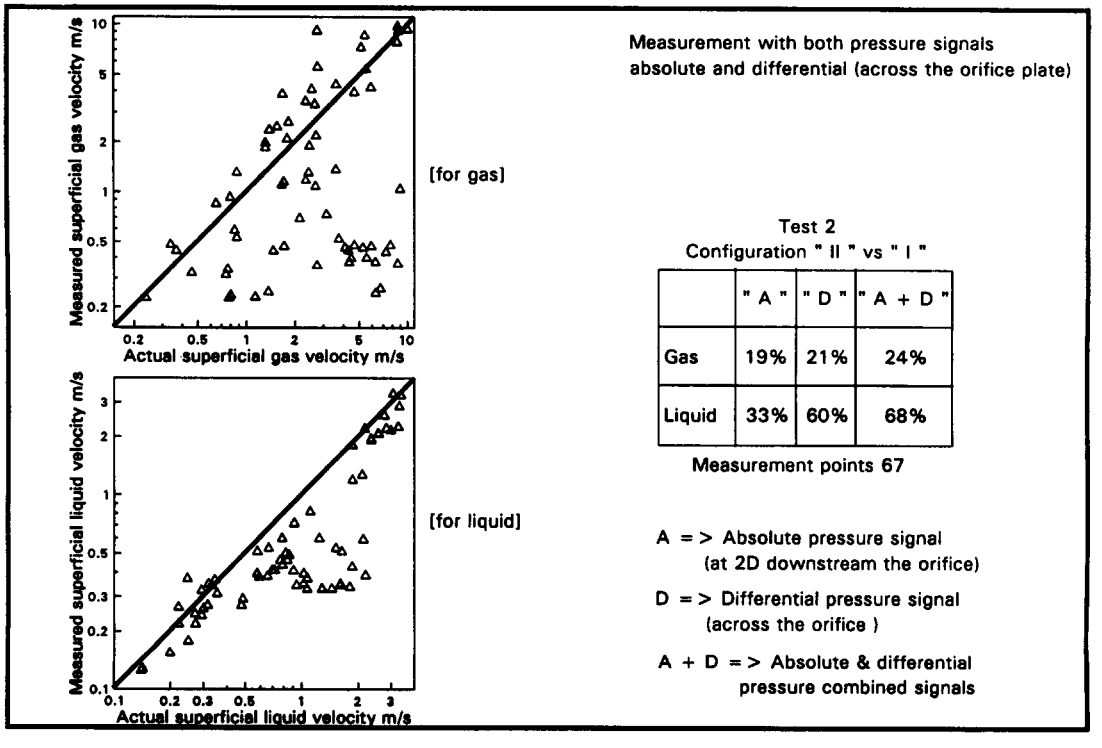

Figure 11. Measuring accuracy (Test 2, configurations II vs I).

As before, the template-matching technique was used in these measurements. The measurement accuracy was very poor, as shown in figure 11, demonstrating a strong upstream installation effect on the measuring accuracy.

However, an interesting secondary conclusion can be drawn from the present study regarding recovery lengths by comparison of the F-ratios (figure 7). It appears that flow recovery takes place over a shorter distance downstream on the Statiflo mixer than a simple step expansion. This conclusion is reached because of the higher F-ratios at the same downstream locations from the Statiflo mixer (configuration III) compared with the step expansion (configuration II).

The S values for configurations II vs I resulted in a higher value (0.285) than that for configurations I vs I (0.131), as shown in figure 8. Thus, it could be concluded that configurations II vs I exhibited a stronger dissimilarity than that which was accountable for by a straight reproducibility test.

4.3. Test 3. Off-site Calibration With a Homogenizer

Measurements in this test series were designed to evaluate the measuring accuracy of the technique used with an off-site calibration database when the detecting sensors are shielded from upstream disturbances by homogenization.

A set of 80 measurements was obtained in configuration IV (with step expansion to simulate disturbance and a homogenizer to isolate the effect of the disturbance). The calibration database was built from configuration III (straight pipe with a homogenizer).

The template-matching technique was used to test 80 measurements against configuration III's database. The measurement accuracy was as good as that obtained in Test 1, and is shown in figure 12.

Figure 8 shows that the S value of configurations IV vs III (0.162) was very close to that for configurations III vs III (0.159). Therefore, it could be concluded that the introduction of the Statiflo mixer had a beneficial effect on the flow recovery length. This is demonstrated by the decrease in the Similarity Scale value and the increase in the F-ratio in moving from the configuration with just a step expansion (configuration II) to the configuration with a step expansion plus the Statiflo mixer (configuration IV).

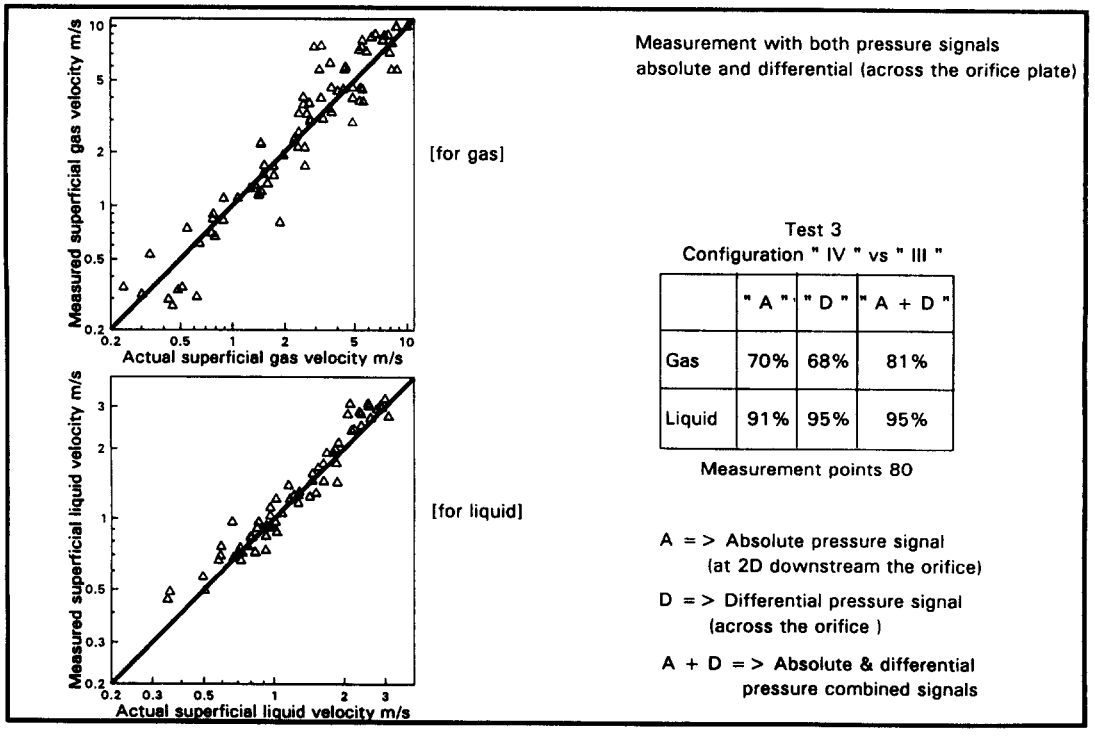

Figure 12. Measuring accuracy (Test 3, configurations IV vs III).

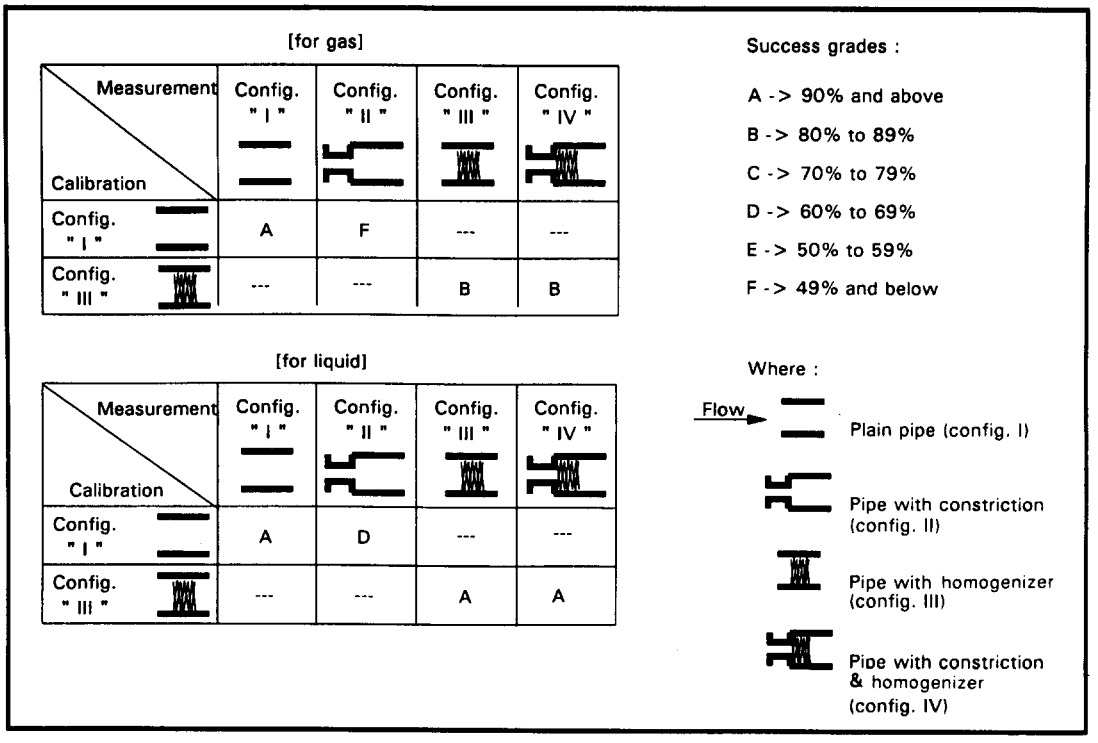

Figure 13. Measurement accuracy summary.

Finally, the small erosion in the Similarity Scale and F-ratio in moving from the configuration with a homogenizer only (configuration III) to the configuration with a step expansion plus a homogenizer (configuration IV) demonstrates the effectiveness of the homogenizer.

5. CONCLUSIONS

The superficial gas–liquid velocity surface can be divided into grid cells where each cell can be uniquely characterized by a set of stochastic features derived from the turbulent hydrodynamic waveforms (e.g. differential and absolute pressure signals). The individual phase velocities can be measured by the template-matching pattern recognition technique.

The results of the three tests are summarized in figure 13, where the recognition rate was graded into bands from "A" (>90% of the measurements are identified with an accuracy of better than $\pm 10\%$) to "F" (<49% of the measurements are identified with an accuracy of better than $\pm 10\%$). It is seen that measurements with off-site calibration with homogenization get a "B" for gas and an "A" for liquid measurements. Measurement with on-site calibration gets a double "A". The off-site calibration without homogenization fails with "F" for gas and "D" for liquid measurements.

The effectivness of the homogenizer in shielding the flowmeter from installation effects was quantified with reference to the Similarity Scale. The F-ratio and Similarity Scale can also be used to determine the optimum location of the detection sensors.

The technique can be extended to oil–water–gas three-phase flow with advances in the following directions:

- Incorporating sensors sensitive to the hydrodynamic/physical properties of the three phases (i.e. in addition to the current pressure sensors such as capacitance and γ-ray densitometer).
- Introduction of new hydrodynamic systems (at present it is the superficial gas and liquid velocities) for scaling of the pipe diameter and fluid properties.

- Use of neural network pattern recognition techniques that take into consideration the sensitivity/resilience of the feature-sets to the flow regime and fluid properties, and compensate for the relative strengths of the features by weighting coefficients. Some success has already been achieved in this direction.

REFERENCES

ASHKURI, S. & HILL, T. J. 1985 Measurement of multi-phase flows in crude oil production systems. *Pet. Rev.* **39,** 14–16.

ATAL, B. S. 1976 Automatic recognition of speakers from their voices. *Proc. IEEE* **64,** 349–364.

DARWICH, T. D., TORAL, H. & ARCHER, J. S. 1991 A software technique for flowrate measurement in horizontal two-phase flow. *SPE Prod. Engng* **6,** 265–270.

KING, C. H., OUYANG, M. S., PEI, B. S. & WANG, Y. W. 1988 Identification of two-phase flow regimes by an optimum modelling method. *Nucl. Technol.* **82,** 211–226.

KOUBA, G. E., SHOHAM, O. & BRILL, J. P. 1990 A non-intrusive flowmetering method for two-phase intermittent flow in horizontal pipes. *SPE Prod. Engng* **5,** 373–380.

LU, Z. Q. & WANG, M. J. 1991 Application of statistical pattern recognition method to identification of two-phase flow pattern and the transition. In *Proc. Int. Conf. Multi-phase Flows '91*, Tsukuba, Japan, pp. 33–36.

MAKHOUL, J. 1975 Linear prediction: a tutorial review. *Proc. IEEE* **63,** 561–580.

MANDHANE, J. M., GREGORY, G. A. & AZIZ, K. 1974 A flow pattern map for gas–liquid flow in horizontal pipes. *Int. J. Multiphase Flow* **1,** 537–553.

MATSUI, G. 1985 Identification of flow patterns in horizontal gas–liquid two-phase flow using differential pressure fluctuations. In *Proc. Int. Symp. on Fluid Control and Measurement*, Tokyo, Japan, pp. 819–824.

MAZZONI, A., BASSITI, K., GIULIANI, F. & BENETTI, M. 1991 The development of a subsea well testing system. In *Proc. 5th Int. Conf. of Multi-phase Production*, Cannes, France, pp. 403–419.

SEKOGUCHI, K., INOUE, K. & IMASAKA, T. 1987 Void signal analysis and gas–liquid two-phase flow regime determination by a statistical pattern recognition method. *JSME Int. J.* **30,** 1266–1273.

TORAL, H., BEG, N. & ARCHER, J. S. 1990 Multi-phase flowmetering by software. *Int. Conf. on Basic Principles & Industrial Applications of Multiphase Flow*, London, U.K.

VINCE, M. A. & LAHEY, R. T. 1982 On the development of an objective flow regime indicator. *Int. J. Multiphase Flow* **8,** 93–124.